IMPUTATION OF RAMP FLOW DATA USING THE ASYMMETRIC CELL TRANSMISSION TRAFFIC FLOW MODEL

Ajith Muralidharan *

Department of Mechanical Engineering
University of California
Berkeley, California 94720
Email: ajith@berkeley.edu

Roberto Horowitz

Department of Mechanical Engineering
University of California
Berkeley, California 94720
Email: horowitz@berkeley.edu

ABSTRACT

The Asymmetric Cell Transmission model can be used to simulate traffic flows in freeway sections. The model is specified by fundamental diagram parameters- determined from mainline data, and on-ramp and off-ramp flows. The mainline flow/density data are efficiently archived and readily available, but the ramp flow data are generally found missing. This paper presents an imputation technique based on iterative learning control to determine these flows. The imputation technique is applied sequentially on all the segments of the freeway, and the ramp flows, which minimize the error between the model calculated densities/flows and measurements are investigated. The stability and convergence of the density and flow errors using the imputation updates is also presented. Finally an example is shown to illustrate its use in a practical scenario.

1 INTRODUCTION

Traffic flow simulations using models provide cheap and tunable tools to study the operation of a freeway. These models can be used to study benefits of different improvement strategies like ramp metering and demand management. First order models, especially the Cell transmission models (CTM) [1] are used frequently to simulate traffic flows and design control strategies. The asymmetric cell transmission model [2] is a modified version of the CTM, particularly suited to simulating traffic flows in freeways. CTMSIM [3] is an interative tool in Matlab which simulates the freeway operation using the ACTM.

*Address all correspondence to this author.

Traffic flow simulations using the ACTM requires the freeway model to be specified with parameters and inputs. The essential parameters include the fundamental diagram for the freeway sections while the inputs are typically on-ramp flows and off-ramp flows/split ratios. The model is specified / calibrated to re-create the basic operation of the freeway observed on any particular day. The veracity of the model/simulation technique is usually established by good conformation of different simulated quantities (E.g. Flows and speeds) with the measured data. California freeways are equipped with loop detector based vehicle detector stations, which record flow, velocity and occupancy data at their location. PeMS [4] is an online archival tool that stores these data. The fundamental diagram can be specified using the flow and density measurements from the mainline vds (positioned along the freeway). The onramp flows and offramp flows are specified by the flow data obtained from the ramp detector data, if available. Ramp flow data is typically found missing over some segments and sometimes even over entire critical sections of the freeway. Thus, in order to specify a simulation model, imputation (estimation) of these ramp flows gain importance.

Traditionally, short term prediction/imputation of missing data in loop detectors has been investigated using various techniques like time series analysis [5] and Kalman filters [6]. Recently, Chen et.al [7] have used a linear regression based imputation procedures to successfully predict missing data in freeway mainline loop detector stations over long periods. This method cannot be applied to impute missing data in on-ramp or off-ramp vehicle detector stations, since we cannot guarantee a high correlation of data between neighboring ramp loop detector stations.

Hence, model based imputation procedures are required to determine missing ramp flow data. In [8, 9], ramp flow imputation algorithms have been proposed using the Link Node Cell Transmission model. [10] proposes an imputation algorithm using the ACTM. Though these algorithms have been successfully applied for ramp flow imputation, no proof of stability/convergence is currently available for these algorithms.

This paper introduces a new iterative learning based adaptive identification of the ramp flows using the ACTM. A rigorous stability/convergence proof of the proposed algorithm is presented using a Lyapunov functional approach. The proof is constructive in that it points to a number of significant additions and modifications that must be introduced to the algorithm presented in [10] in order to satisfy the conditions imposed by the stability/convergence analysis, which in turn enhance the performance of the algorithm. Section 2 contains a short review of the ACTM used for freeway corridor simulation. Section 3 presents the imputation algorithm used for determining ramp flows. Section 4 analyzes the stability and convergence of the imputation procedure. Finally, Section 5 demonstrates the imputation algorithm on data from a small section of the I-210W freeway in the Los Angeles area.

2 ASYMMETRIC CELL TRANSMISSION MODEL

This section presents a short summary of the ACTM [2]. The freeway is specified as a sequence of segments, each with a on-ramp near the beginning of the section and an off-ramp near the end of the section. Figure 1 shows the freeway divided into N sections or cells, where vehicles move from left to right. Boundary conditions can be specified in different ways. Vehicles can be specified to enter the freeway through an on-ramp while the downstream end is assumed to be in free-flow (BC-1). Another variation of BC-1 assumes the downstream to be in free-flow, while the upstream flow is directly fed into the freeway through a queue. Density of the cells upstream of the first section and downstream of the last section can also be specified as the boundary conditions for simulation (BC-2). While BC-2 is appropriate to simulate the base scenario, BC-1 is preferred for simulation, especially under ramp control, since the control strategy usually modifies the densities at the boundaries. It must be noted that BC-1 places restrictions on the freeway sections chosen for simulation, since the beginning and end of the freeway section simulated should always be in free-flow. Table 1 lists the model variables and parameters. Each section of the freeway is characterized by a fundamental diagram (Figure 2) which specifies its traffic flow characteristics. The section length are absorbed in the fundamental diagram parameters for convenience.

The ACTM is a time and space discretization of the Lighthill-Whitham-Richards (LWR) equation. Thus the ACTM can also

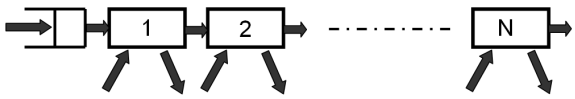

Figure 1. FREEWAY WITH N SECTIONS.

Symbol	Name	Units
F_i	maximum flow (capacity) of section i	veh/period
v_i	free flow speed of section i	section/period
w_i	congestion wave speed of section i	section/period
n_i^c	critical density of section i	veh/section
n_i^J	jam density of section i	veh/section
$f_i(k)$	flow from section i to $i+1$ at period k	veh/period
$s_i(k), r_i(k)$	off-ramp, on-ramp flow in section i at period k	veh/period
$n_i(k)$	number of vehicles in section i at period k	veh/section
$Q(k)$	number of vehicles in the input queue to section 1 at period k	veh
$f_{in}(k)$	input flow at upstream queue at period k	veh/period

Table 1. MODEL VARIABLES AND PARAMETERS.

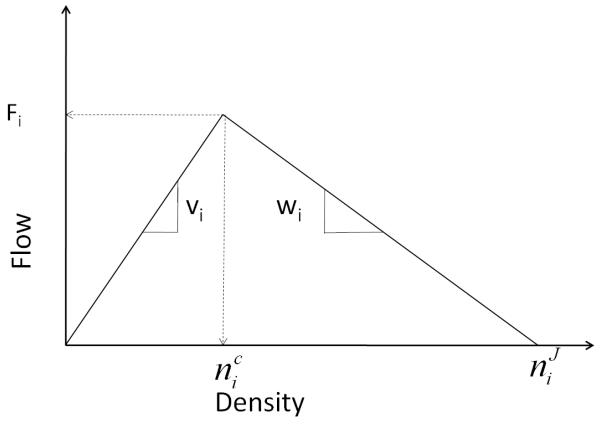

Figure 2. FUNDAMENTAL DIAGRAM OF SECTION i.

be represented as a continuous time spatially discretized model, as presented here. Also, the general model can be specified with off-ramp flows or off-ramp split ratios. We will consider the version with off-ramp flows, as these flows can also be converted easily to split ratios. Also, we will consider the variation of BC-1 where the upstream flow is directly fed into the freeway through a queue.

The following equations describe the model.

$$\begin{aligned}
&\dot{n}_i(k) = f_{i-1}(k) - f_i(k) + r_i(k) - s_i(k), \quad 1 \le i \le N \\
&f_i(k) = \min(v_i n_i(k) - s_i(k), w_{i+1}[n^J_{i+1} - n_{i+1}(k)], F_i) \quad 1 \le i < N \\
&f_N(k) = \min(v_N n_N(k) - s_N(k), F_N) \\
&f_0(k) = \min(w_1[n^J_1 - n_1(k)], Q(k) + f_{in}(k)) \\
&Q(k+1) = Q(k) + f_{in}(k) - f_0(k)
\end{aligned} \tag{1}$$

When density boundary conditions (n_0 and n_{N+1}) are specified, the model is specified as

$$\begin{aligned}
&\dot{n}_i(k) = f_{i-1}(k) - f_i(k) + r_i(k) - s_i(k) \quad 1 \le i \le N \\
&f_i(k) = \min(v_i n_i(k) - s_i(k), w_{i+1}[n^J_{i+1} - n_{i+1}(k)], F_i) \quad 1 \le i \le N
\end{aligned} \tag{2}$$

where w_{N+1} and n^J_{N+1} are the congestion wave speed and jam density of the cell directly following the boundary. The flow $f_i(k)$ is said to be in free-flow if

$$v_i n_i(k) - s_i(k) < \min[w_{i+1}[n^J_{i+1} - n_{i+1}(k)], F_i] \tag{3}$$

and otherwise it is in congestion. With respect to each section, the in flow (from upstream) can be either in free-flow or in congestion and the out flow (to downstream section) can also be either in congestion/freeflow. In each of the four cases, the density and the flow equations can be combined to a single update equation. Thus the model can also be represented using a four mode model.

3 IMPUTATION ALGORITHM

The imputation algorithm presented in this section is based on the ACTM. Typically, mainline flow and density profiles are available from PeMS. Ramp flows are imputed such that the density and flow profiles with the estimated ramp data match the actual measurements from the freeway. The procedure has been extended from the adaptive iterative identification technique described in [11, 12]. It is assumed that the density and ramp flow profile is 24 hour periodic, and the on-ramp and off-ramp flows are represented as a convolution of a kernel on a constant periodic ramp parameter (influence) vector.

$$r(k) = \int_0^T K_r(\tau,k) c_r(\tau) d\tau, \quad s(k) = \int_0^T K_s(\tau,k) c_s(\tau) d\tau \tag{4}$$

where $K_r(\tau,k)$ and $K_s(\tau,k)$ represent periodic, time dependent kernel functions with period T, which is also the period of the process considered. Some typical kernel functions include an impulse or a gaussian window centered at time k. Kernel function width is chosen with respect to the degree of smoothness expected from the imputed profile. A short kernel window (eg. an impulse function) will lead to noisy estimations as compared to a kernel with a large window.

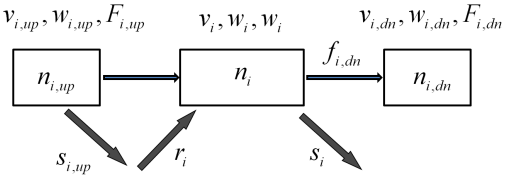

Figure 3. IMPUTATION PARAMETERS AND CELL DEFINITIONS

The structure of the ACTM allows us to decouple the estimation of ramp flows. The imputation is carried out section by section sequentially, starting from the most upstream section 1. For estimation of section i ramp flows, we consider the immediate upstream section $i-1$ and the immediate downstream section $i+1$. The upstream (downstream) section is specified with the subscript up (dn). Figure 3 shows the parameters and measurement data used for imputation of ramp flows in section i. The upstream boundary conditions includes the upstream density, fundamental diagram parameters as well as the off-ramp flow $s_{i,up}$. The imputation proceeds sequentially from upstream to downstream and either $s_{i,up}$ or its estimate is available. Since all the parameters and variables carry the subscript i, for clarity, we drop it in the following equations.

Traffic data $n_{up}(k)$, $n(k)$, $n_{dn}(k)$, $s_{up}(k)$ and $f_{dn}(k)$ and ramp flows $r(k)$ and $s(k)$ are assumed to be periodic with period $T = 24 hours$. These assumptions are not restrictive, as the freeway is observed to be in free flow, with low densities at midnight. Thus, unknown on-ramp and/or off-ramp flows are estimated indirectly by estimating their respective influence coefficients $\hat{c_r}$ and $\hat{c_s}$ using a repetitive adaptive learning algorithm [11, 12], which runs continuously cycling through the 24 hour traffic data.

For each section, the imputation procedure assumes initial estimates for the ramp parameter functions $\hat{c_r}$ and $\hat{c_s}$. These estimates are then adapted so that the model calculated densities match with the density profile recorded in the vehicle detector station. Let P represent Plant (i.e the actual system described using the ACTM) while M represent the Model, calculated using the estimates. The model variables and the estimates are represented with a $\hat{}$ ($\hat{n}, \hat{r}$ etc.) and the errors with a $\tilde{}$ (e.g. $\tilde{n}(k) = n(k) - \hat{n}(k)$, where $n(k)$ is the section's measured number of vehicles and $\hat{n}(k)$ is the number of vehicles generated by the model at instant k). The actual variables are represented without

any accent. Table 2 presents the various modes considered in the imputation where

$$\bar{w}_{dn}(k) = min\left(\frac{F}{n^J_{dn} - n_{dn}(k)}, w\right) \tag{5}$$

is introduced in order to absorb the capacity flow into the congestion mode.The modes considered here only refer to the flow conditions downstream (i.e out of the section considered), i.e $P-F$ and $P-C$ correspond to free-flow and congested flow conditions downstream respectively.

Symbol	Condition
$P-F$	$f_{dn}(k) < \bar{w}_{dn}(k)[n^J_{dn} - n_{dn}(k)]$
$P-C$	$f_{dn}(k) = \bar{w}_{dn}(k)[n^J_{dn} - n_{dn}(k)]$
$M-F$	$v\hat{n}(k) - \hat{s}(k) < \bar{w}_{dn}(k)[n^J_{dn} - n_{dn}(k)]$
$M-C$	$v\hat{n}(k) - \hat{s}(k) > \bar{w}_{dn}(k)[n^J_{dn} - n_{dn}(k)]$

Table 2. PLANT AND MODEL MODES.

The mode dependent adaptation laws for the parameters at each step are given by

(a) P-F , M-F (plant and model are both in free-flow downstream)

$$\begin{aligned}\dot{\hat{c}}_r(\tau,k) &= G_1 K_r(\tau,k)\tilde{n}(k)\\ \dot{\hat{c}}_s(\tau,k) &= -G_2 K_s(\tau,k)\tilde{f}_{dn}(k)\end{aligned} \tag{6}$$

(b) P-C , M-C (plant and model are both in congestion downstream)

$$\begin{aligned}\dot{\hat{c}}_r(\tau,k) &= G_1 K_r(\tau,k)\tilde{n}(k)\\ \dot{\hat{c}}_s(\tau,k) &= -G_1 K_s(\tau,k)\tilde{n}(k)\end{aligned} \tag{7}$$

(c) P-C , M-F (plant is in congestion and model is in free flow downstream)

$Case(i) \qquad \tilde{n}(k) > 0$

$$\begin{aligned}\dot{\hat{c}}_r(\tau,k) &= G_1 K_r(\tau,k)\tilde{n}(k)\\ \dot{\hat{c}}_s(\tau,k) &= -G_1 K_s(\tau,k)\tilde{n}(k) - G_2 K_s(\tau,k)\frac{\tilde{f}_{dn}(k) + |\tilde{f}_{dn}(k)|}{2}\end{aligned}$$

$Case(ii) \qquad \tilde{n}(k) \leq 0$

$$\begin{aligned}\dot{\hat{c}}_r(\tau,k) &= G_1 K_r(\tau,k)\tilde{n}(k)\\ \dot{\hat{c}}_s(\tau,k) &= -G_2 K_s(\tau,k)\tilde{f}_{dn}(k)\end{aligned} \tag{8}$$

(d) P-F , M-C (plant is in free flow and model is in congestion downstream)

$Case(i) \qquad \tilde{n}(k) < 0$

$$\begin{aligned}\dot{\hat{c}}_r(\tau,k) &= G_1 K_r(\tau,k)\tilde{n}(k)\\ \dot{\hat{c}}_s(\tau,k) &= -G_1 K_s(\tau,k)\tilde{n}(k) - G_2 K_s(\tau,k)\tilde{f}_{dn}(k)\end{aligned}$$

$Case(ii) \qquad \tilde{n}(k) \geq 0$

$$\begin{aligned}\dot{\hat{c}}_r(\tau,k) &= G_1 K_r(\tau,k)\tilde{n}(k)\\ \dot{\hat{c}}_s(\tau,k) &= -G_2 K_s(\tau,k)\tilde{f}_{dn}(k)\end{aligned} \tag{9}$$

where G's are user defined positive gains.The model density update at each steps is given by

$$\begin{aligned}\tilde{n}(k) &= n(k) - \hat{n}(k)\\ \dot{\hat{n}}(k) &= \hat{f}_u - \hat{f}_d + \hat{r}(k) - \hat{s}(k) - a\tilde{n}(k)\\ \hat{f}_u &= min(n_{up}(k)v_{up} - s_{up}(k), F_{up}, w(n^J - \hat{n}(k)))\\ \hat{f}_d &= min(\hat{n}(k)v - \hat{s}(k), \bar{w}_d n(k)(n^J_{dn} - n_{dn}(k)))\\ \hat{r}(k) &= \int_0^T K_r(\tau,k)\hat{c}_r(\tau,k)d\tau\\ \hat{s}(k) &= \int_0^T K_s(\tau,k)\hat{c}_s(\tau,k)d\tau\end{aligned} \tag{10}$$

$$\tilde{f}_{dn}(k) = f_{dn}(k) - (n(k)v - \hat{s}(k)) \tag{11}$$

The parameter a in (10) is chosen so as to make the error equations asymptotically stable. In the update equations, on-ramp flows are always updated to decrease the density error, and hence the update are proportional to the current density error. The off-ramp flows are either adapted using the the density error (terms with gain G_1) and/or downstream flow error (terms with gain G_2), depending on the mode. This ensures that the downstream flow error also decreases during the imputation.

While the parameter and model density update equations are given in continuous time, the model is implemented in discrete time with a small time step and small gains, so that the imputation procedure as well as the model are stable. Typically the time step Δt is chosen such that $V_{max}\Delta t < 1$, where $V_{max} \geq v_i$ for $i = 1..N$ and v_i is the free flow speed at section i. The adaptation is carried out for the entire density profile multiple times, so as to reduce the 24-hour 'errors' $\sum_k |n(k) - \hat{n}(k)|$ and $\sum_k |f_{dn}(k) - \hat{f}_{dn}(k)|$. This procedure is repeated until both the errors becomes insignificant (eg. $< 0.5\% \quad of \quad \sum_k n(k)$ and $< 0.5\% \quad of \quad \sum_k f_{dn}(k)$) or stops decreasing (eg. change of errors of $< 0.5\% \quad of \quad \sum_k n(k)$ and $< 0.5\% \quad of \quad \sum_k f_{dn}(k)$ across iterations)

4 STABILITY AND CONVERGENCE

In this section, we will study the stability and convergence of the density errors under the adaptation laws given in Section 3. The error equations are given by

$$\begin{aligned}\dot{\tilde{n}}(k) &= \tilde{f}_u(k) - \tilde{f}_d(k) + \tilde{r}(k) - \tilde{s}(k) - a\tilde{n}(k) \qquad (12)\\ \tilde{r}(k) &= \int_0^T K_r(\tau,k)\tilde{c}_r(\tau,k)d\tau\\ \tilde{s}(k) &= \int_0^T K_s(\tau,k)\tilde{c}_s(\tau,k)d\tau\end{aligned}$$

We will also show that the downstream flow converges in all the modes.

The condition stated below will be used in the following lemma and theorems.

Condition 4.1. *For the system described in Figure 3, the following conditions apply:*
(1) $s_{up}(k) = \hat{s}_{up}(k)$ *when the plant upstream is in free-flow.*
(2) $w(n^J - n(k)) < \min(F_{up}, n_{up}(k)v_{up} - \hat{s}_{up}(k)))$ *when the plant upstream is in congestion.*

Condition 4.1 guarantees that the upstream off ramp estimation error $\tilde{s}_{up}(k) = s_{up}(k) - \hat{s}_{up}(k)$ is either zero or it does not affect the upstream (input) flows in the current section. For the freeway described in Figure 1, this condition is easily achieved for the first cell (i=1) and as it will later be shown by induction in Theorem 4.2, it will apply to all cells.

Lemma 4.1. *For the system described by Figure 3, given* n_{up}, $\hat{s}_{up}$, n_{dn}, f_{dn}, n *and the fundamental diagram parameters for all the cells, under Condition 4.1,* $\tilde{f}_u(k) = f_u(k) - \hat{f}_u(k)$ *is given by* $\tilde{f}_u(k) = -\zeta w\tilde{n}(k)$ *where* $0 \le \zeta \le 1$

Proof. Depending on the upstream flow condition in the model and plant, the system falls into four modes.

Case (a) : Plant upstream (F), Model upstream (F)

$$\begin{aligned}f_u(k) &= \min(F_{up}, n_{up}(k)v_{up} - s_{up}(k)))\\ \hat{f}_u(k) &= \min(F_{up}, n_{up}(k)v_{up} - s_{up}(k)))\\ \tilde{f}_u(k) &= 0 \qquad (13)\end{aligned}$$

Case (b) : Plant upstream (F), Model upstream (C)

$$\begin{aligned}f_u(k) &= \min(F_{up}, n_{up}(k)v_{up} - s_{up}(k)))\\ \hat{f}_u(k) &= w(n^J - \hat{n}(k))\\ \tilde{f}_u(k) &= -\zeta w\tilde{n}(k) \qquad 0 \le \zeta \le 1\end{aligned}$$

since

$$w(n^J - n(k)) > \min(F_{up}, n_{up}(k)v_{up} - s_{up}(k))) > w(n^J - \hat{n}(k)) \qquad (14)$$

Case (c) : Plant upstream (C), Model upstream (C)

$$\begin{aligned}f_u(k) &= w(n^J - n(k))\\ \hat{f}_u(k) &= w(n^J - \hat{n}(k))\\ \tilde{f}_u(k) &= -w\tilde{n}(k) \qquad (15)\end{aligned}$$

Case (d) : Plant upstream (C), Model upstream (F)

$$\begin{aligned}f_u(k) &= w(n^J - n(k))\\ \hat{f}_u(k) &= \min(F_{up}, n_{up}(k)v_{up} - \hat{s}_{up}(k)))\\ \tilde{f}_u(k) &= -\zeta w\tilde{n}(k) \qquad 0 \le \zeta \le 1\end{aligned}$$

since

$$w(n^J - n(k)) < \min(F_{up}, n_{up}(k)v_{up} - \hat{s}_{up}(k))) < w(n^J - \hat{n}(k)) \qquad (16)$$

Hence $\tilde{f}_u(k) = -\zeta w\tilde{n}(k)$ where $0 \le \zeta \le 1$, i.e it is a stabilizing term for the error equations.

Theorem 4.1. *For the system described in Figure 3, given* n_{up}, $\hat{s}_{up}$, n_{dn}, f_{dn} , n, *and the fundamental diagram parameters, the parameter updates laws in Section 3 stabilize the error equations (8) when Condition 4.1 applies. Moreover,* $s(k) = \hat{s}(k)$ *when the plant downstream is in free-flow and* $\bar{w}_{dn}(n^J_{dn} - n_{dn}(k)) \le \min(F_{up}, n_{up}(k)v_{up} - \hat{s}_{up}(k)))$ *otherwise.*

Proof. Consider the Lyapunov functional $V(k)$ (and its time derivative) given by

$$\begin{aligned}V(k) &= \frac{1}{2}\tilde{n}(k)^2 + \frac{1}{2G_1}\int_0^T \tilde{c}_r(\tau,k)^2 d\tau + \frac{1}{2G_1}\int_0^T \tilde{c}_s(\tau,k)^2 d\tau\\ \dot{V}(k) &= \tilde{n}(k)\dot{\tilde{n}}(k) + \int_0^T \tilde{c}_r(\tau,k)G_1^{-1}\dot{\tilde{c}}_r(\tau,k)d\tau\\ &\quad + \int_0^T \tilde{c}_s(\tau,k)G_1^{-1}\dot{\tilde{c}}_s(\tau,k)d\tau \qquad (17)\end{aligned}$$

We need to show that $\dot{V}(k)$ is negative semi-definite, for the error equations to be stable.

From lemma 4.1, we see that $\tilde{f}_u(k) = -\zeta w\tilde{n}(k)$ for some $0 \leq \zeta \leq 1$, irrespective of the mode of the plant/model with respect to upstream flow. Hence, the error equations can be simplified into four cases corresponding to the downstream flow. The following equations show that $\dot{V}(k) \leq 0$ in all the four cases.

(i) P-F, M-F

$$\begin{aligned}
\dot{\tilde{n}}(k) &= -\zeta w\tilde{n}(k) - v\tilde{n}(k) + \int_0^T K_r(\tau,k)\tilde{c}_r(\tau,k)d\tau \\
\dot{\tilde{c}}_r(\tau,k) &= -G_1K_r(\tau,k)\tilde{n}(k) \\
\dot{\tilde{c}}_s(\tau,k) &= G_2K_s(\tau,k)\tilde{f}_{dn}(k) = -G_2K_s(\tau,k)\tilde{s}(k) \\
\dot{V}(k) &= -(a+v+\zeta w)\tilde{n}(k)^2 + \tilde{n}(k)\int_0^T K_r(\tau,k)\tilde{c}_r(\tau,k)d\tau - \\
&\quad \tilde{n}(k)\int_0^T K_r(\tau,k)\tilde{c}_r(\tau,k)d\tau - \frac{G_2}{G_1}\tilde{s}(k)^2 \leq 0
\end{aligned} \tag{18}$$

(ii) P-F, M-C
In this case $n(k)v - s(k) \leq \bar{w}_{dn}(n^J_{dn} - n_{dn}(k)) \leq \hat{n}(k)v - \hat{s}(k)$,

$$\begin{aligned}
\dot{\tilde{n}}(k) &= -(\zeta w+a)\tilde{n}(k) - n(k)v + s(k) + \bar{w}_{dn}(n^J_{dn} - n_{dn}(k)) \\
&\quad + \tilde{r}(k) - \tilde{s}(k) \\
&= -(\zeta w + a + v)\tilde{n}(k) - \hat{n}(k)v + \hat{s}(k) + \bar{w}_{dn}(n^J_{dn} - n_{dn}(k)) \\
&\quad + \tilde{r}(k)
\end{aligned}$$

$(a) \quad \tilde{n}(k) < 0$

$$\begin{aligned}
\dot{\tilde{c}}_r(\tau,k) &= -G_1K_r(\tau,k)\tilde{n}(k) \\
\dot{\tilde{c}}_s(\tau,k) &= G_1K_s(\tau,k)\tilde{n}(k) + G_2K_s(\tau,k)\tilde{f}_{dn}(k) \\
\dot{V}(k) &= -(a+\zeta w)\tilde{n}(k)^2 - \tilde{n}(k)(n(k)v - s(k) - \bar{w}_{dn}(n^J_{dn} - \\
&\quad n_{dn}(k))) + \tilde{n}(k)\tilde{r}(k) - \tilde{n}(k)\tilde{s}(k) - \tilde{n}(k)\tilde{r}(k) \\
&\quad + \tilde{n}(k)\tilde{s}(k) - \frac{G_2}{G_1}\tilde{s}(k)^2 \leq 0
\end{aligned}$$

$(b) \quad \tilde{n}(k) \geq 0$

$$\begin{aligned}
\dot{\tilde{c}}_r(\tau,k) &= -G_1K_r(\tau,k)\tilde{n}(k) \\
\dot{\tilde{c}}_s(\tau,k) &= G_2K_s(\tau,k)\tilde{f}_{dn}(k) \\
\dot{V}(k) &= -(a+\zeta w+v)\tilde{n}(k)^2 - \tilde{n}(k)(\hat{n}(k)v - \hat{s}(k) - \bar{w}_{dn}(n^J_{dn} \\
&\quad - n_{dn}(k))) + \tilde{n}(k)\tilde{r}(k) - \tilde{n}(k)\tilde{r}(k) - \frac{G_2}{G_1}\tilde{s}(k)^2 \leq 0
\end{aligned} \tag{19}$$

(iii) P-C, M-F
In this case $\hat{n}(k)v - \hat{s}(k) \leq \bar{w}_{dn}(n^J_{dn} - n_{dn}(k)) \leq n(k)v - s(k)$,

$$\begin{aligned}
\dot{\tilde{n}}(k) &= -(\zeta w+a)\tilde{n}(k) - \bar{w}_{dn}(n^J_{dn} - n_{dn}(k)) + \hat{n}(k)v - \hat{s}(k) \\
&\quad + \int_0^T K_r(\tau,k)\tilde{c}_r(\tau,k)d\tau - \int_0^T K_s(\tau,k)\tilde{c}_s(\tau,k)d\tau \\
&= -(\zeta w + a + v)\tilde{n}(k) - \bar{w}_{dn}(n^J_{dn} - n_{dn}(k)) + n(k)v - s(k) \\
&\quad + \int_0^T K_r(\tau,k)\tilde{c}_r(\tau,k)d\tau
\end{aligned}$$

$(a) \quad \tilde{n}(k) > 0$

$$\begin{aligned}
\dot{\tilde{c}}_r(\tau,k) &= -G_1K_r(\tau,k)\tilde{n}(k) \\
\dot{\tilde{c}}_s(\tau,k) &= G_1K_s(\tau,k)\tilde{n}(k) + G_2K(k)\frac{\tilde{f}_{dn}(k) + |\tilde{f}_{dn}(k)|}{2} \\
\dot{V}(k) &= -(a+\zeta w)\tilde{n}(k)^2 - \tilde{n}(k)(\bar{w}_{dn}(n^J_{dn} - n_{dn}(k)) - \hat{n}(k)v \\
&\quad + \hat{s}(k)) + \tilde{n}(k)\tilde{r}(k) - \tilde{n}(k)\tilde{s}(k) - \tilde{n}(k)\tilde{r}(k) + \tilde{n}(k)\tilde{s}(k) \\
&\quad + \frac{G_2}{G_1}\tilde{s}(k)\frac{\tilde{f}_{dn}(k) + |\tilde{f}_{dn}(k)|}{2} \leq 0
\end{aligned}$$

$(b) \quad \tilde{n}(k) \leq 0$

$$\begin{aligned}
&\dot{\tilde{c}}_r(\tau,k) = -G_1K_r(\tau,k)\tilde{n}(k) \\
&\dot{\tilde{c}}_s(\tau,k) = G_2K_s(\tau,k)\tilde{f}_{dn}(k) \geq 0 \\
&Also, 0 \geq \tilde{n}(k)v \geq \tilde{s}(k) \\
&\dot{V}(k) = -(a+\zeta w+v)\tilde{n}(k)^2 - \tilde{n}(k)(\bar{w}_{dn}(n^J_{dn} - n_{dn}(k)) - n(k)v \\
&\quad + s(k)) + \tilde{n}(k)\tilde{r}(k) - \tilde{n}(k)\tilde{s}(k) - \tilde{n}(k)\tilde{r}(k) + \tilde{s}(k)\tilde{f}_{dn}(k) \leq 0
\end{aligned} \tag{20}$$

(iv) P-C, M-C

$$\begin{aligned}
\dot{\tilde{n}}(k) &= -\zeta w\tilde{n}(k) + \int_0^T K_r(\tau,k)\tilde{c}_r(\tau,k)d\tau - \int_0^T K_s(\tau,k)\tilde{c}_s(\tau,k)d\tau \\
\dot{\tilde{c}}_r(\tau,k) &= -G_1K_r(\tau,k)\tilde{n}(k) \\
\dot{\tilde{c}}_s(\tau,k) &= G_1K_s(\tau,k)\tilde{n}(k) \\
\dot{V}(k) &= -(a+\zeta w)\tilde{n}(k)^2 + \tilde{n}(k)\int_0^T K_r(\tau,k)\tilde{c}_r(\tau,k)d\tau - \\
&\quad \tilde{n}(k)\int_0^T K_s(\tau,k)\tilde{c}_s(\tau,k)d\tau - \tilde{n}(k)\int_0^T K_r(\tau,k)\tilde{c}_r(\tau,k)d\tau \\
&\quad + \tilde{n}(k)\int_0^T K_s(\tau,k)\tilde{c}_s(\tau,k)d\tau \leq 0
\end{aligned} \tag{21}$$

Therefore the Lyapunov function $V(k)$ is bounded and decreasing, and thereby $\tilde{n}(k)$,$\tilde{c}_r(\tau,k)$,$\tilde{c}_r(\tau,k)$ are bounded. $\ddot{V}(k)$ can be expressed as a function of $\tilde{n}(k)$,$\tilde{c}_r(\tau,k)$, $\tilde{c}_s(\tau,k)$ and other bounded terms in all the four cases listed above and therefore can be shown to be bounded. Hence by Barbalats' lemma, $\dot{V}(k) \to 0$

as $k \to \infty$. Analyzing $\dot{V}(k)$, we see that $\tilde{n} = 0$ at equilibrium. Also, when Plant is in free-flow, $\tilde{s}(k) = 0$ and when Plant is in congestion $\hat{n}(k)v - \hat{s}(k) \geq \bar{w}_{dn}(n^J_{dn} - n_{dn}(k))$. This also implies that $\tilde{f}_d = 0$.

The results derived for the above system with density boundary conditions also apply with other boundary conditions. The following theorem states the applicability of the sequential imputation procedure described in Theorem 4.1 to a multi-section freeway.

Theorem 4.2. *For the freeway described by Figure 1, given the upstream & downstream boundary conditions, density,flow measurements and fundamental diagram parameters of all the sections, we can impute the ramp flows sequentially from upstream to downstream section-wise using the update laws described in Section 3. In all the sections,* $\tilde{f}_{i,d} = 0$ *and* $\tilde{n}_i = 0$.

Proof. For the first section, since upstream boundary conditions are given, the imputation ensures $\tilde{f}_{1,d} = 0$ and $\tilde{n}_1 = 0$, and $\hat{s}_1$ satisfies the Condition 4.1. We can see that for any section i, given measurement data and upstream off-ramp flow estimate satisfying Condition 4.1, the imputation algorithm ensures $\tilde{f}_{i,d} = 0$, $\tilde{n}_i = 0$ after imputation. Moreover, the imputed off-ramp flow, which forms the upstream boundary condition for section $i+1$ satisfy Condition 4.1 by Theorem 4.1. This proves the theorem by induction.

5 EXAMPLES

The imputation algorithm is demonstrated with two examples. In the first example, artificial data is used to generate density profiles in a 1 section freeway with density boundary conditions, with known on-ramp and off-ramp flows. Then these ramp flows (assumed unknown) are imputed using the imputation algorithm. Figure 4 shows the result of the imputation. Both the flow and the density have converged during the imputation. However, in some time segments the on-ramp and the off-ramp values have not converged to their true values. These segments correspond to the P-C M-C mode, and in this case, the ramp flows are not individually observable. In fact, there are infinitely many combinations of on-ramp and off-ramp flows in the P-C M-C mode corresponding to the observed density.

In the second example, a 9.8 mile highway section from I-210W was chosen. This freeway section was divided into 10 sections with 10 on-ramps and 7 off-ramps, out of which 6 on-ramps and 3 off-ramps were imputed. The imputed data was used to simulate the traffic flow in the entire freeway. The density, flow and velocity contours of the simulation are shown in Figure 5. The

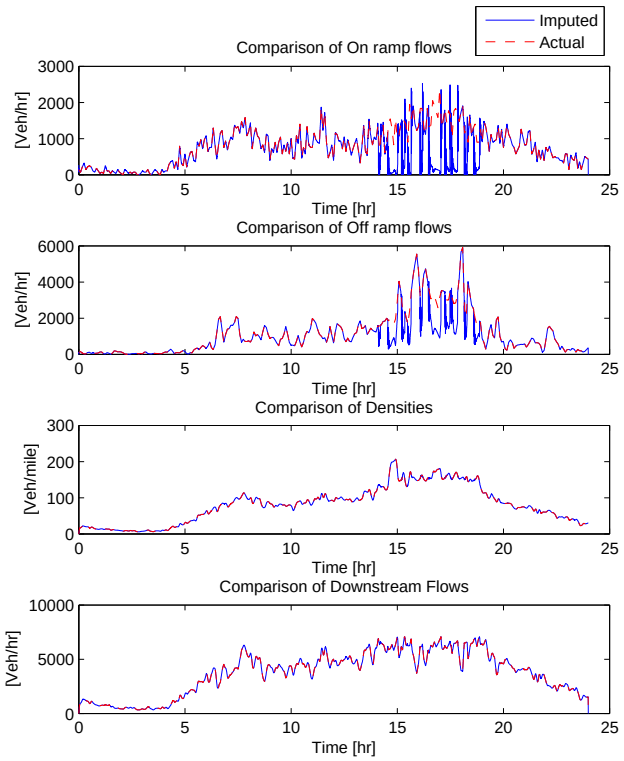

Figure 4. Results of the Imputation with artificial data.

X-axis of the contours represent Postmiles, which measure distance along the freeway, and the Y-axis represents the time of the day. The density and flow error of the simulation is 12.13 % and 13.29 % respectively. It was observed that in many sections, the imputation stopped converging and the solutions showed significant errors in Flow and density. This implies that there exists no plausible ramp flows that correspond to the data available, which indicate faulty mainline data/ramp data. This indicates the potential use of the imputation algorithm in fault detection in mainline data.

6 CONCLUSION

This paper describes an imputation algorithm based on the ACTM, to estimate ramp flow data in freeways. The unknown ramp flows are represented as a convolution of a known time varying kernel function with a constant influence/parameter function. Thus the imputation procedure was reduced to estimation of these constant influence functions. Parameter update equations, based on iterative learning control techniques, were presented. These parameter update stabilize the density error equations and the density and flow error converge to 0. The first example presented in Section 5 showed that the flow and

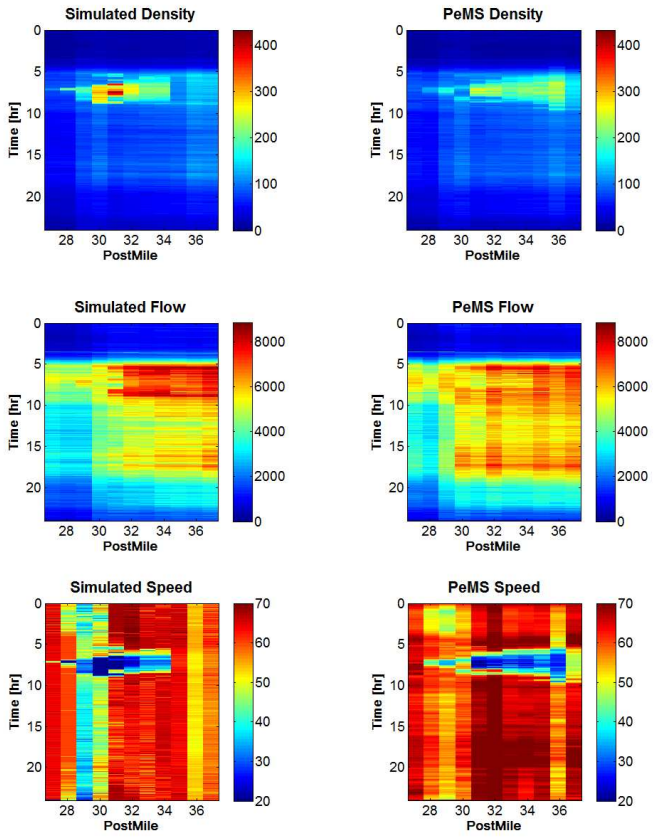

Figure 5. Simulation results for I-210W.

density errors converge to zero. The second example illustrated the application of the algorithm in a small stretch of the I-210W freeway. In this case, the flow and density errors converged to non-zero values which were significant. Since the imputation algorithm, with correct measurements should lead to zero density and flow errors, the non-zero errors after convergence show incorrect flow/density measurements. Thus the imputation procedure can be extended for detecting faults.

The algorithm presented in this paper results in zero density and flow errors (ideally) after imputation. In comparison, the algorithms presented in [10], [9] need not always result in zero flow errors. Also, the algorithm presented here can be used to easily identify faults in data as compared to the imputation algorithm based on the Link Node CTM [9] since the imputation algorithm is decoupled section-wise, enabling easy identification/isolation of faulty segments.

ACKNOWLEDGMENT

This work is supported by the California Department of Transportation through the California PATH Program. The contents of this paper reflect the views of the author and not necessarily the official views or policy of the California Department of Transportation.

REFERENCES

[1] Daganzo, C., 1994. "The cell transmission model: A dynamic representation of highway traffic consistent with the hydrodynamic theory". *Transportation Research, Part B*, **28**(4), pp. 269–287.

[2] Gomes, G., and Horowitz, R., 2006. "Optimal freeway ramp metering using the asymmetric cell transmission model". *Transportation Research, Part C*, **14**(4), pp. 244–262.

[3] Kurzhanskiy, A., 2007. "Modeling and software tools for freeway operational planning". PhD thesis, University of California, Berkeley.

[4] PeMS, 2007. PeMS website. http://pems.eecs.berkeley.edu, accessed 8/28/2007.

[5] Jacobson, L., Nihan, N., and Bender, J., 1990. "Detecting erroneous loop detector data in a freeway traffic management system". In Transportation Research Record 1287, TRB, National Research Council, pp. 151–166.

[6] Dailey, D., 1993. Improved error detection for inductive loop sensors. Tech. Rep. WA-RD 3001, Washington State DOT, May.

[7] Chen, C., Kwon, J., Rice, J., Skabardonis, A., and Varaiya, P., 2003. "Detecting errors and imputing missing data for single loop surveillance systems". In Transportation Research Record, Vol. 1855, TRB, National Research Council, pp. 160–167.

[8] Muralidharan, A., Dervisoglu, G., and Horowitz, R., 2009. "Freeway traffic flow simulation using the cell transmission model". Proceedings of the American Control Conference, St. Louis.

[9] Muralidharan, A., and Horowitz, R., 2009. "Imputation of ramp flow data for freeway traffic simulation". Accepted for publication in Transportation Research Records,2009.

[10] et al., A. C., 2008. Topl: Tools for operational planning of transportation networks. Presented at the Dynamic systems and control conference, 2008.

[11] Messner, W., Horowitz, R., Kao, W.-W., and Boals, M., 1991. "A new adaptive learning rule". *IEEE Transactions on Automatic Control*, **36-2**, pp. 188–197.

[12] Horowitz, R., Messner, W., and Moore, J. B., 1991. "Exponential convergence of a learning controller for robot manipulators". *IEEE Transactions on Automatic Control*, **36-7**, pp. 890–892.